Acoustic emission characteristics of PM-PCF vibration sensor for Structural Health Monitoring of Composite

Zheng He, Xiaoyu Sun [a, *], Xuan Gu, Qingbo Sui, Ju Liu, Kuo Yuan

College of Aerospace and Civil Engineering, Harbin Engineering University, Harbin 150001 China

[a]sunxiaoyu520634@163.com

Abstract

In the present work, Structural Health Monitoring (SHM) of a composite beam using embedded Polarization Maintaining Photonic Crystal Fiber (PM-PCF) has been investigated with emphasis on better monitoring of composite materials and the wide range of potential applications this class of materials currently have. This new concept of using PM-PCF for SHM is attractive because it enables the design of a vibration sensor that is highly sensitive to vibration and at the same time is insensitive to temperature. Vibration measurements up to 50 Hz have been demonstrated in this work.

Keywords

Vibration measurement; Polarization Maintaining Photonic Crystal Fiber; Composite materials; Structural Health Monitoring.

1. Introduction

Monitoring and detection of damage in structures at an early stage is very important in a number of applications where, for example, vibrations may lead to structural or mechanical failure.Dynamic loading of a structure gives rise to induced vibrations、which generally occur at a frequency close to the natural frequency of the structure, potentially resulting in severe damage to the structure in certain situations. In particular, the knowledge of the vibration characteristics plays an important role in the detection and identification of structural damage. The dynamic response of the structure viz. obtaining information on the vibration amplitude and its frequency are important in case of aeronautical structures[1].

In this work, the time domain response/temporal characteristics of the response of an embedded FOS have been acquired and then transformed into the frequency domain to obtain the information required on the vibration response of the composite. In the present research, the use of an embedded FOS-based PM-PCF is proposed for sensor applications and evaluated for the detection of the relevant vibration parameters in the composite structures under study.Further, the embedded sensor has been tested in terms of the use for response in different scenarios – to sine, square and triangular temporal profiles of the applied vibrations.

2. Sensor Design

Fig. 1(a) shows a schematic diagram of the set-up used for vibration sensing in a Glass Fiber Reinforced Polymer (GFRP) using an embedded PM-PCF, while Fig. 1(b) shows the photograph of the actual system and the set-up itself. The PM-PCF is made up of single material i.e. pure silica with diameter of 250 m which includes an acrylate coating, with a cladding diameter of 125 m with a holey region of 40 m. It has air holes in the cladding region running along the fiber of diameter 2.2 m which gives the lower effective refractive index in comparison to that in the solid core. The spacing between air holes is 4.4 m. Two bigger air holes of diameter 4.5 m are present and adjacent to the core to give the circular asymmetry of the effective refractive index distribution and hence the form birefringence. The cross section of the PM-PCF used is as shown in Fig. 2.

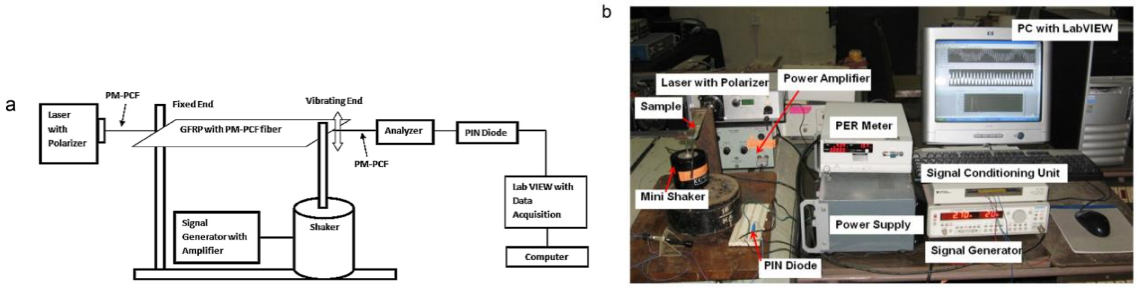

Fig. 1. (a) Schematic of the experimental setup and (b) a photograph showing the system used.

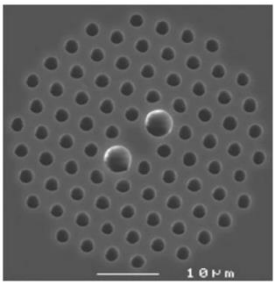

Fig. 2. Cross section of the PMPCF used .

For the fabrication of the glass composite specimen, unidirectional glass fabric was used as a reinforcement system in the epoxy resin matrix (LY 1564, Araldite) with suitable hardener (Aradur 3486, Araldite). A 60% weight fraction was used for the reinforcement and matrix system. All the fabric layers were put in the 0. direction and special care has been taken to avoid crossed or angled layers of fabric. It consists of 8 plies with a length of 150 mm, a width of 23 mm and a thickness of 2.5 mm. The PM-PCF is embedded after the 2nd ply from the bottom surface as shown in Fig. 3 using the hand-lay-up method with vacuum bagging process [2]. The ends of the fiber have been protected by inserting them in small rubber tubes. The total length of the fiber is 650 mm.

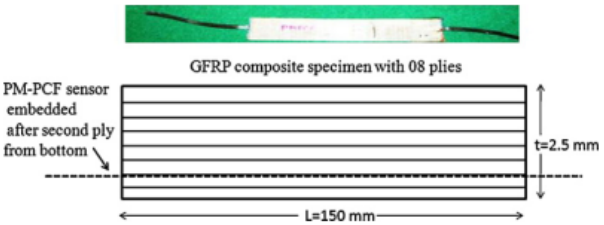

Fig. 3. Glass composite specimen: a photograph (upper) and its schematic (lower).

3. Results And Discussion

The embedded sensor has been tested to evaluate its use in response to different scenarios – to sinusoidal, triangular and square temporal profiles of the applied vibrations. The sensor has been tested in the frequency range of 1–50 Hz, in steps of 0.5 Hz. Fig. 4(a–c) shows the time domain response of the sensor signal for input sinusoids of frequencies 1 Hz, 20 Hz and 50 Hz, as representative plots. Fig. 5(a–c) shows the corresponding FFT analysis of the acquired optical signal, from which it can clearly be seen that there is a good agreement between the applied signal and the detected sensor signal at these different frequencies. The sensor has given a clear frequency response up to 20 Hz in the time and frequency domain. It is apparent from the figures that, at higher frequencies (which is >20 Hz), the sensor signal does not give a readable information but its FFT response clearly indicates the detected frequency of the sensor. For an excitation frequency of 50 Hz, noisy time domain and frequency domain signals were obtained. In the frequency domain, some frequency components in the range of 1–20 Hz along with a dominant peak at 50 Hz were observed. For this reason, the frequency range axis has been limited to 20–60 Hz,as shown in Fig. 5(c).

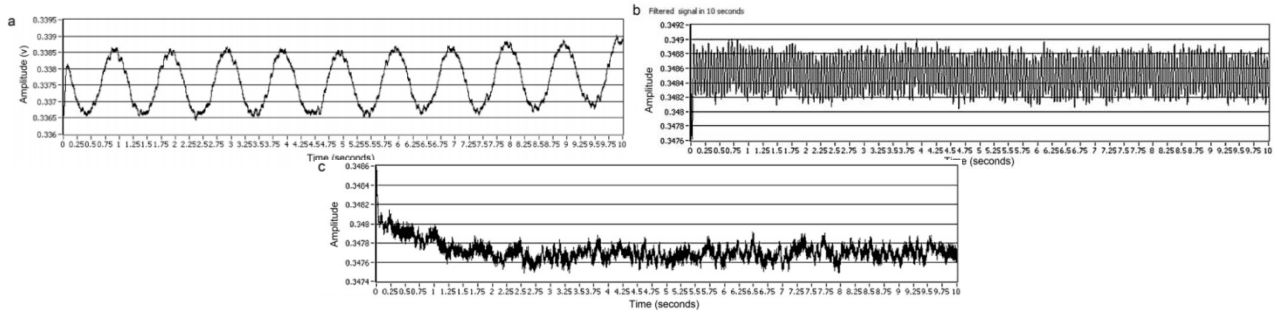

Fig. 4. Sinusoidal sensor signal at excitation frequencies of (a) 1 Hz (b) 20 Hz and (c) 50 Hz.

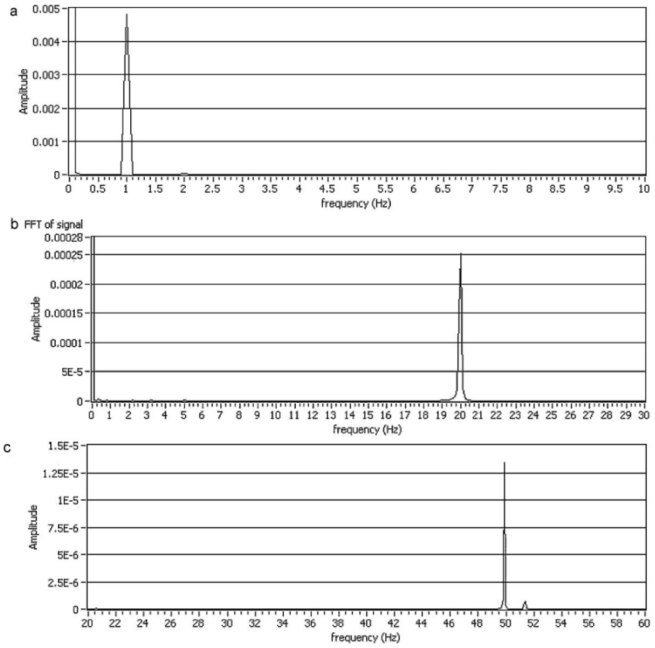

Fig. 5. FFT of the sinusoidal sensor signal indicating a detected frequency of (a) 1 Hz, a small noise component is also visible at 51.4 Hz, (b) 20 Hz and (c) 50 Hz.

The time domain signal and the corresponding FFT signal from the sensor for a triangular input function of frequencies 1 Hz and 50 Hz are shown in Figs. 6(a and b) and 7(a and b). These results have indicated the feasibility of the sensor for vibration sensing up to 50 Hz with a resolution of 0.5 Hz. Results obtained in this case are similar to those found for the case of sinusoidal excitation of the sample.The sensor response has also been evaluated for a square wave function which is very important for a different application, i.e. in a rotating machinery diagnosis system. For the square wave profile,the specimen has only been excited up to 5 Hz due to the maximum load limitation of mini shaker. Fig. 8(a and b) shows the time domain signal for the square input function of frequency of 1 Hz and 5 Hz whereas Fig. 9(a and b) shows the corresponding FFT. It is worth mentioning that the difference between the square and sine wave excitation lies in the generation of harmonics for the square wave which has not been achieved for the sine wave. The presence of harmonics arises due to the nonlinear excitation of the sample with the square wave excitation [3].

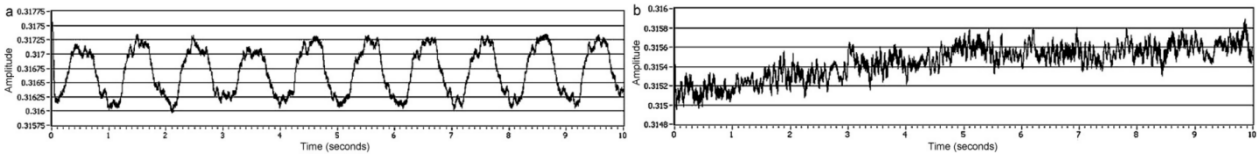

Fig. 6. Triangular sensor signal at excitation frequency of (a) 1 Hz and (b) 50 Hz.

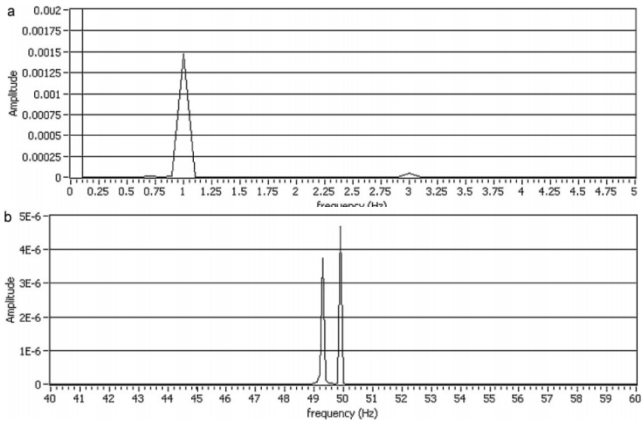

Fig. 7. FFT of the triangular sensor signal indicating a detected frequency of (a) 1 Hz and (b) 50 Hz.

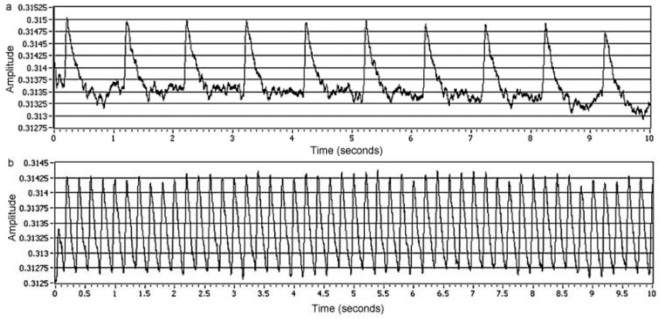

Fig. 8. Square sensor signal at an excitation frequency of (a) 1 Hz and (b) 5 Hz.

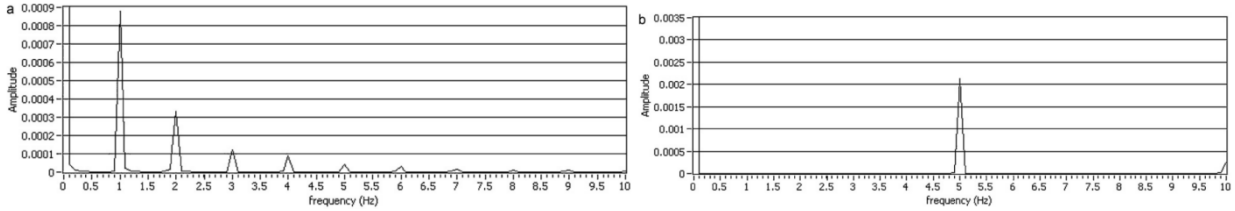

Fig. 9. FFT of square sensor signal indicating a detected frequency of (a) 1 Hz and (b) 5 Hz with harmonics of decreasing amplitude.

In order to determine the sensitivity of the device, the amplitude variation of the FFT of the sensor response has been plotted as a function of the input voltage applied to the mini shaker to allow its excitation and this is shown in Fig. 10. The figure has been plotted for the following three frequencies viz. 1 Hz, 5 Hz and 10 Hz. A linear relationship of obtained amplitude with excitation voltage is clearly seen in the figure. Similar results have been obtained by Chan et al.[4]. The sensitivity of the sensor has been found to be 30.12 × 10-6 per volt at 1 Hz, 15.36 × 10-6 per volt at 5 Hz and 30.85 × 10-6 per volt at 10 Hz.

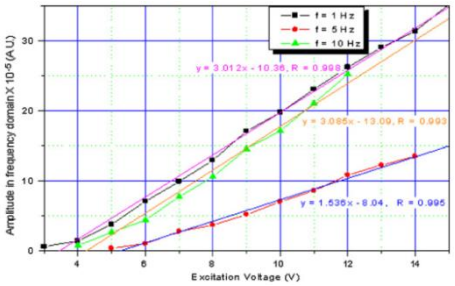

Fig. 10. Amplitude in frequency domain as a function of the excitation voltage at 1 Hz, 5 Hz and 10 Hz.

In order to analyze the frequency response of the embedded PMPCF sensor, the amplitude variation of the FFT peak corresponding to sensor response to the applied frequency to the shaker has been plotted as shown in Fig. 11. The obtained response is not linear which means that the embedded

sensor response can be obtained clearly in the frequency range of 1–20 Hz, which has been discussed in earlier section. A similar behavior for the frequency response curve has been reported by Kumar et al. [5] and Zhang and Bao[6].

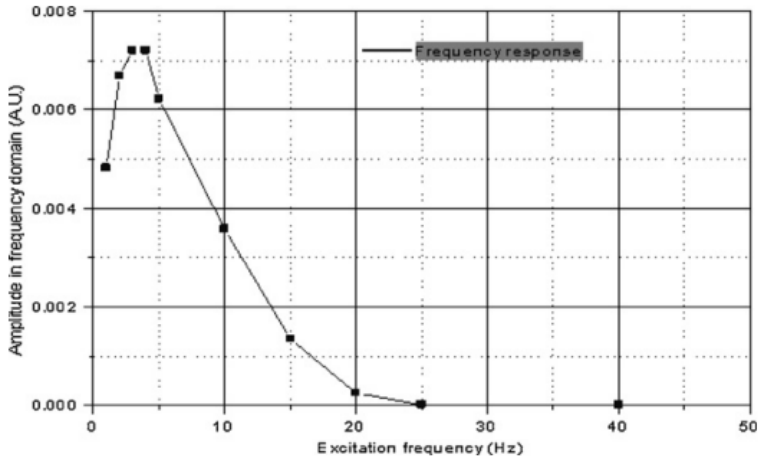

Fig. 11. Frequency response of the PM-PCF sensor at an excitation voltage 8 V.

The sensor response has been validated with reference to a conventional piezoelectric accelerometer (Bruel & Kjaer type 4366).The displacement has been measured using an accelerometer as well as a traveling microscope, as shown in Fig. 12. It gives the first natural frequency of the specimen at the peak displacement,which occurs at a frequency of ~30 Hz. The accelerometer signal has been integrated twice to calculate the displacement. Suitable band-pass filters have been used to filter out the DC component,which comes out after the integration. Fig. 13 shows the FFT plot of the output of the accelerometer at an excitation frequency of 10 Hz and voltage of 8 V, while Fig. 14 shows the amplitude in the frequency domain at 5 Hz, as a function of the excitation voltage.

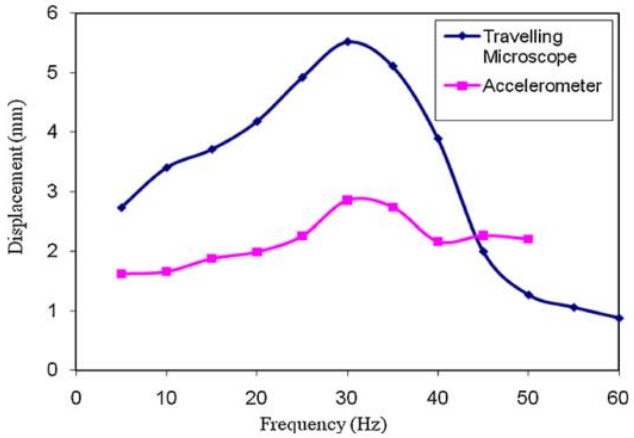

Fig. 12. Displacementmeasured using travelingmicroscope (upper) and accelerometer (lower) vs. frequency of GFRP beam.

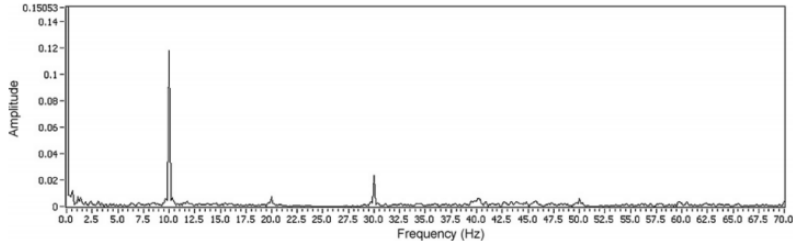

Fig. 13. FFT plot of the output of the accelerometer at an excitation voltage of 8 V and an excitation frequency of 10 Hz.

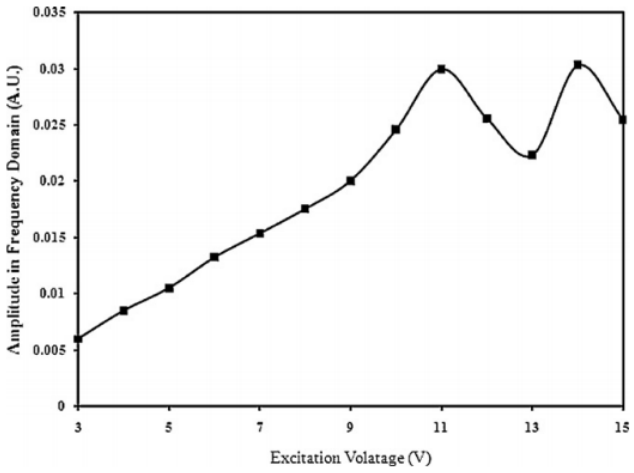

Fig. 14. Amplitude in frequency domain as a function of excitation voltage at 5 Hz for the accelerometer.

Fig. 15 compares the temperature dependence of the nonembedded PM-PCF sensor with that of conventional polarization maintaining 'Panda' fiber of the same length embedded in the same environment. It clearly indicates that the PM-PCF sensor has also an added advantage over the conventional polarization maintaining 'Panda' fiber when used over the measured temperature range,in terms of its temperature independence. The origin of the temperature independence is because of the single material composition i.e. silica in the PM-PCF, while the Panda fiber is made up of different materials. Because of the difference in thermal expansion coefficients of the materials comprising the Panda fiber, there is a considerable change in stress birefringence due to temperature and hence the Panda fiber becomes more sensitive to temperature changes, a deleterious effect in most sensors [7]. Hence, PM-PCF based sensors may potentially find applications in harsh environments where there are considerable temperature excursions and where the minimum temperature–vibration cross coupling is desirable.

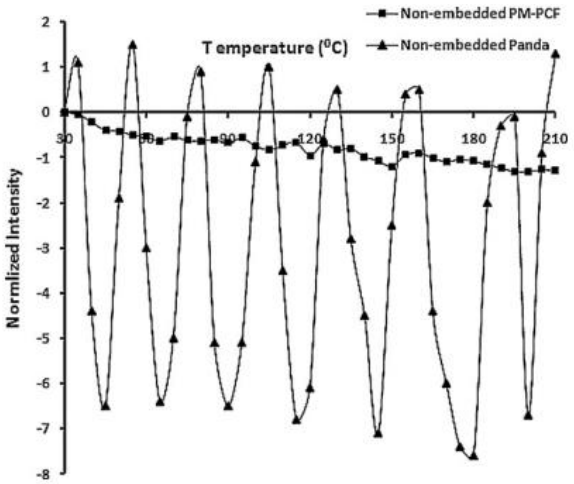

Fig. 15. Intensity variations with respect to change in temperature for (a) PM-PCF and (b) Panda fiber.

4. Conclution

In the present work, the application of a PM-PCF used for SHM applications, characterized by embedding it in a glass composite, has been demonstrated for the first time and a vibration analysis of the same structure has been carried out. The advantages of using a long gauge PM-PCF sensor, based on the polarimetric–interferometric technique, have been seen and comments on the performance characteristics addressed. The sensor has been tested in the frequency range of 1–50 Hz using excitation signals of various types and it may find application in vibration measurements of larger structures.

Acknowledgements

This work is supported by the National Natural Science Foundation of China（No. 11602066） and the National Science Foundation of Heilongjiang Province of China (QC2015058 and 42400621-1-15047), the Fundamental Research Funds for the Central Universities.

References

[1] S.W. Doebling, C.R. Farrar, M.B. Prime, A summary of vibration-based damage identification methods, Shock Vib. Dig. 30 (1998) 91–105.
[2] F.L.Matthews, Rees D. Rawlings, CompositeMaterials: Engineering and Science, Woodhead, England, 1999, pp. 133–135.
[3] J.L. Taylor, The Vibration Analysis Handbook, first ed., VCI, 2003, p. 17.
[4] H.L.W. Chan, K.S. Chiang, J.L. Gardner, Polarimetric optical fiber sensor for ultrasonic power measurement, in: IEEE-Ultrasonics Symposium, 1988, pp.599–602.
[5] P. Kumar, N. Chandrasekaran, M. Gerg, Fiber optic sensor for localized vibration measurement, in: 7th International Conference on Optoelectronics, Fiber Optics and Photonics, 2004.
[6] Z. Zhang, X. Bao, Continuous and damped vibration detection based on fiber diversity detection sensor by Rayleigh backscattering, J. Lightwave Technol. 26(2008) 832–838.
[7] C.L. Zhao, X. Yang, C. Lu, W. Jin, M.S. Demokan, Temperature-insensitive interferometer using a highly birefringent photonic crystal fiber loop mirror, IEEE Photon. Technol. Lett. 16 (2004) 2535–2537.